



Strut Thickness But Not Unit Cell Length Alters Mechanical Properties of 3D Printed Rib Implants: A Preliminary Study

Richa Gupta, BS¹
 Lauren Judkins, BS²
 Christine Gabriele²
 Charles Tomonto, PhD³
 Guha Manogharan, PhD²
 Michael W. Hast, PhD¹

¹University of Pennsylvania, Philadelphia, PA

²The Pennsylvania State University, State College, PA

³Johnson and Johnson 3D Printing

Introduction

Chest flail injuries, where two or more ribs are fractured, are painful injuries which can lead to long-term disability and even mortality¹. Open reduction internal fixation with titanium plates and screws is commonly used to reduce these fractures but this technique has undesirable clinical outcomes, with up to 15% of patients requiring revision surgery². Changing the mechanical properties of implants with additive manufacturing techniques may allow us to address patient-specific needs, which ultimately improves clinical outcomes. In large additively manufactured parts, it is known that changing strut thickness and unit cell length of a lattice (Figure 1) can effectively change mechanical properties^{3,4,5,6}. However, little is known about how lattice architecture of rib implants influences mechanical properties of the implant—primarily because they are only 1.5 mm thick. The purpose of this study was to investigate how discrete changes to strut thickness and unit cell length change mechanical properties of titanium rib implants in bending (Figure 1). We hypothesized that altering the strut thickness and unit cell length of the lattice would lead to significant changes in bending stiffness and yield load.

Methods

24 test coupons that were similar width and thickness of existing rib fracture fixation plates (100 x 10 x 1.5 mm) were printed with a medical grade titanium alloy (Ti-6Al-4V Grade 23) powder. 20 coupons had 5 different lattice structures (n = 4) and solid coupons were used as the control (n = 4) (Figure 1). Test coupons had a shell thickness of 0.25 mm, and a 1 mm thick internal lattice section. For the lattice structures, unit cell length ranged from 1-3 mm, and strut thickness ranged from 0.225-0.425mm, which resulted in porosities ranging from 36-86%. External surfaces of the plates were designed with 13 holes (1 mm diameter) to allow powder drainage after manufacturing. All specimens were subjected to stress relief via heat treatment prior to testing. The geometric qualities and surface characteristics were evaluated via scanning electron microscopy (SEM). 4-point

bending tests were performed to evaluate mechanical properties of each design. Tests were performed at 1.3 mm/min in a universal test frame with 25 mm spans between support and compression anvils. Bending stiffness, yield load, bending strength, toughness, post-yield energy, and maximum load were calculated⁷. Results were tested for normality followed by one-way ANOVAs and pairwise comparisons to determine statistical significance (p < 0.05).

Results

Changes in strut thickness and unit cell length led to significant changes in bending stiffness (Figure 2A), max load, and toughness, but no significant changes to yield load (Figure 2B) or bending strength were found. The most porous group (S225L3) exhibited a bending stiffness of 32.8 ± 1.4 N/mm, whereas the least porous group (S425L1) had a value of 38.4 ± 0.4 N/mm (p < 0.001) (Figure 2A). The bending stiffness for control specimens was in the middle of this range (34.8 ± 1.5 N/mm). Similarly, maximum load increased from 286.2 ± 3.3 N in the most porous group to 339.1 ± 6.2 N in the least porous group (p = 0.002), while the control group had a value of 322.0 ± 12.1 N. S225L1

Group Names	Lattice Cross Section	Strut Thickness (mm)	X-direction unit cell length (mm)	Porosity (%)
S225 L3		0.225	3	86
S225 L2		0.225	2	84
S225 L1		0.225	1	78
S325 L1		0.325	1	58
S425 L1		0.425	1	36
Control		N/A	N/A	0

Figure 1. Cartoon diagram of the 5 different lattice cross sections used in this study. Strut thickness ranged from 0.225 to 0.425 mm and unit cell length ranged from 1 to 3 mm.

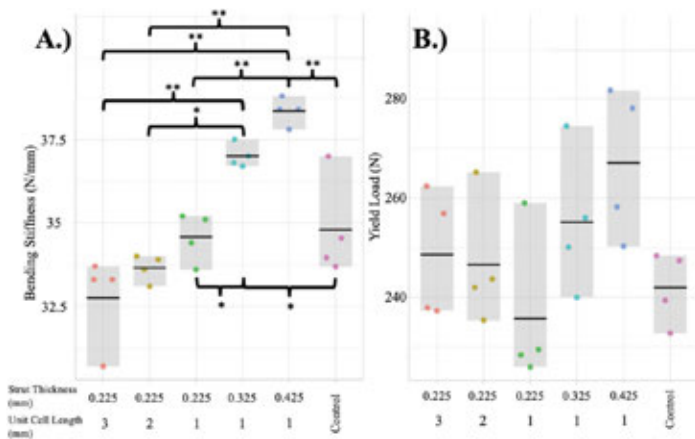


Figure 2. Bending Stiffness and Yield Load results for the 5 heat-treated lattice cross section designs and control specimens. (*) and (**) denotes a statically significant difference between two groups ($p < 0.05$ and $p < 0.001$, respectively).

exhibited the lowest toughness ($5.0 \pm 0.4 \text{ J/mm}^3$), while S425L1 had the highest toughness ($9.7 \pm 2 \text{ J/mm}^3$, $p < 0.001$), while the control was $9.2 \pm 0.3 \text{ J/mm}^3$. Measures of yield load (between $235.7 \pm 15.6 \text{ N}$ and $267.1 \pm 15.2 \text{ N}$) and bending strength (between 2946.6 ± 194.8 and $3338.5 \pm 190.4 \text{ Nmm}$) indicated no significant differences between groups. Finally, SEM images revealed successful formation of a lattice structure around each drainage hole, with some small agglomerations of powder clusters around the rim (Figure 3).

Discussion

Results of this study rejected our hypothesis, that changing both strut thickness and unit cell length would have a significant impact on mechanical properties. Our findings suggest that changing the lattice structure of a thin plate does not elicit the same changes in mechanical properties as cubic structures tested in previous experiments^{4,6}. These preliminary results suggest that alterations to lattice structure can effectively modulate bending stiffness of a rib implant to be greater than or less than a solid control. At the same time, changes to lattice architecture does not significantly impact yield load. When taken together, this means that porous implants may bend more easily but resist permanent deformation at similar loads as their stiffer counterparts. Further testing is needed for refined, full-sized implant designs that include holes for screw placement. Future designs will also incorporate internal gradient-based lattice designs that seamlessly alter mechanical properties along the length of the implant.

Significance/Clinical Relevance

This study provides insight into our ability to fundamentally alter rib fracture implant performance by changing the

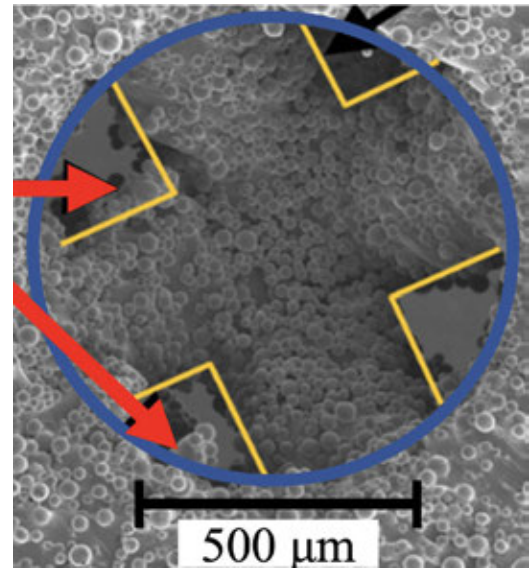


Figure 3. Representative SEM image of drainage hole (blue circle) with struts joining at node (yellow lines), and small powder agglomerations (red arrows).

internal lattices of additively manufactured parts. Future implant designs can leverage this approach to improve congruency between implants and native bone, which may reduce incidence of revision surgery and improve overall clinical outcomes.

Acknowledgements

DePuy Synthes provided materials and technical support for this study.

References

1. Fabricant PD, Robles A, Downey-Zayas T, et al. Development and Validation of a Pediatric Sports Activity Rating Scale: The Hospital for Special Surgery Pediatric Functional Activity Brief Scale (HSS Pedi-FABS). *The American Journal of Sports Medicine*. 2013;41(10):2421-2429.
2. Bottlang M, Walleser S, Noll M, et al. Biomechanical rationale and evaluation of an implant system for rib fracture fixation. *Eur J Trauma Emerg Surg*. 2010;36(5):417-426.
3. Bai L, Gong C, Chen X, et al. Additive Manufacturing of Customized Metallic Orthopedic Implants: Materials, Structures, and Surface Modifications. *Metals*. 2019; 9(9):1004.
4. Mazur, M., Leary, M., Sun, S. et al. Deformation and failure behaviour of Ti-6Al-4V lattice structures manufactured by selective laser melting (SLM). *Int J Adv Manuf Technol*. 2016; 84, 1391-1411.
5. Refai K, Montemurro M, Brugger C, et al. Determination of the effective elastic properties of titanium lattice structures. *Mechanics of Advanced Materials and Structures*. 2020; 27:23, 1966-1982.
6. McKown S, Shen Y, Brookes WK, et al. The quasi-static and blast loading response of lattice structures. *International Journal of Impact Engineering*. 2008; 35(8):795-810. doi:https://doi.org/10.1016/j.ijimpeng.2007.10.005
7. Standard Specification and Test Method for Metallic Bone Plates. *ASTM F382-17*. 2017.